JCTC Journal of Chemical Theory and Computation

Universal Theoretical Approach to Extract Anisotropic Spin Hamiltonians

Rémi Maurice,*[,†,§] Roland Bastardis,[‡] Coen de Graaf,[§,⊥] Nicolas Suaud,[†] Talal Mallah,[||] and Nathalie Guihéry*[,†]

Laboratoire de Chimie et Physique Quantiques, IRSAMC/UMR5626, Université de Toulouse III, 118 route de Narbonne, F-31062 Toulouse Cédex 4, France, Laboratoire de Mathématiques, Physiques et Systemes, Université de Perpignan Via Domitia, 52 Avenue Paul Alduy, 66860 Perpignan, France, Departament de Química Física i Inorganica, Universitat Rovira i Virgili, Marcel lí Domingo s/n, 43007 Tarragona, Spain, Institut de Chimie Moléculaire et des Matériaux d'Orsay, Université Paris sud 11, 91405 Orsay, France, and Institució Catalana de Recerca i Estudis Avançats (ICREA), Passeig Lluis Companys 23, 08010, Barcelona, Spain

Received June 27, 2009

Abstract: Monometallic Ni(II) and Co(II) complexes with large magnetic anisotropy are studied using correlated wave function based ab initio calculations. Based on the effective Hamiltonian theory, we propose a scheme to extract both the parameters of the zero-field splitting (ZFS) tensor and the magnetic anisotropy axes. Contrarily to the usual theoretical procedure of extraction, the method presented here determines the sign and the magnitude of the ZFS parameters in any circumstances. While the energy levels provide enough information to extract the ZFS parameters in Ni(II) complexes, additional information contained in the wave functions must be used to extract the ZFS parameters of Co(II) complexes. The effective Hamiltonian procedure also enables us to confirm the validity of the standard model Hamiltonian to produce the magnetic anisotropy of monometallic complexes. The calculated ZFS parameters are in good agreement with high-field, high-frequency electron paramagnetic resonance spectroscopy and frequency domain magnetic resonance spectroscopy data. A methodological analysis of the results shows that the ligand-to-metal charge transfer configurations must be introduced in the reference space to obtain quantitative agreement with the experimental estimates of the ZFS parameters.

1. Introduction

The recent interest for information storage at the molecular scale motivates both experimental and theoretical studies of molecules presenting a bistability. Among the different bistable chemical systems, single molecule magnets (SMMs)[1−5] are the smallest species that have been conceived. Their remarkable properties come from their intrinsic feature to present two high spin states of different magnetization $+M_S$ and $-M_S$ separated by an energy barrier. From a fundamental point of view, works on these systems have opened new perspectives in the study of quantum mechanics effects such as tunnelling, coherence, and interference. Magnetic anisotropy is responsible for both the existence of the energy barrier and the dominant factor of the tunnelling, and hence, it determines the magnetic behavior of these systems. A crucial landmark for chemistry, for technological devices as well as for fundamental investigations, would be the control and tuning of the magnetic anisotropy.

From a theoretical point of view, the understanding of the electronic and the structural factors governing the anisotropy

* Corresponding author. Telephone: +33561556488. E-mail: rmaurice@irsamc.ups-tlse.fr.
† Université de Toulouse III.
§ Universitat Rovira i Virgili.
‡ Université de Perpignan Via Domitia.
⊥ Institució Catalana de Recerca i Estudis Avançats (ICREA).
|| Université Paris.

10.1021/ct900326e CCC: $40.75
Published on Web 10/02/2009

is of primary importance. The first attempts to calculate anisotropy parameters from first principles are less than 10 years old. Most of the studies concern one component density functional theory (DFT) based calculations with a perturbative inclusion of spin−orbit (SO) coupling (see the ORCA[6−11] and NRLMOL[12−16] code). Very recently, a two-component DFT method[17] has been implemented in the ReSpect code[18] and used to study the zero field splittings (ZFS) of several mononuclear complexes. For polynuclear systems, good agreement with experimental values was obtained using the NRLMOL method for the calculated D and E ZFS parameters of the Fe_4, Mn_{12}, and Mn_6-based SMMs.[19,20] Nevertheless, only the global ZFS parameters of the SMMs in its ground spin states (i.e., the parameters of the giant spin Hamiltonian) were accessible within the DFT scheme. The understanding and control of the property requires studying the local anisotropies of each metal ion and the anisotropies of their interactions. To extract such quantities, the multideterminantal descriptions are mandatory, and the excited spin states should be calculated. Wave function based calculations can provide this accurate description of the multideterminantal character of SMMs wave functions, but only few works dealt with the extraction of ZFS parameters using wave function based computational schemes. One can mention the pioneering work of Michl[21] involving a perturbative treatment of spin dependent terms and the work done by Ågren et al.[22] based on the linear response theory. Among the most popular methods, we quote the ones implemented in the ORCA[6] and MOLCAS[23] codes. Both codes provide accurate results on the mono- and polynuclear nuclear complexes.[7−11,24−28]

In the present paper, spin-orbit restricted active space state interaction (SO-RASSI) calculations on mononuclear species are performed in order to determine the energies and wave functions of the lowest electronic states. These solutions are then used to build and to calculate the matrix elements of the effective Hamiltonian that best fits the ab initio results. Since this Hamiltonian matrix can be compared to the commonly used model Hamiltonian matrix, the procedure provides a rational way to check (and eventually to improve) the ability of the phenomenological Hamiltonian to describe accurately the magnetic anisotropy. The same philosophy has been applied to many magnetic systems in order to measure the different contributions to the magnetic exchange integral[29,30] and to rationally parametrize t-J models,[31,32] double exchange models,[33−39] and spin Hamiltonians.[40] In all cases, the procedure has shown the validity and the application limits of the phenomenological Hamiltonians that are commonly used to interpret the experimental data or to understand the physics of the system under study. The comparison has led to different improvements of the model Hamiltonians, such as the inclusion of a priori neglected exchange interactions,[31] and the three- or four-body operators[41,42] that are crucial for the reproduction of the magnetic properties of the systems. Concerning the study of magnetic anisotropy, the effective Hamiltonian theory is particularly promising for polynuclear species given the uncertainties in the proper definition of the model Hamiltonian for these systems.[43−45] In this work, we use the effective Hamiltonian theory to extract the anisotropic spin Hamiltonian from the first principles for mononuclear species, laying in this way, the foundation for the study of the more complicated polynuclear systems. We show how the magnetic anisotropy axes can be determined, and that the rigorous computational extraction of the anisotropy parameters for the high spin d^7 configuration requires the construction of an effective Hamiltonian.

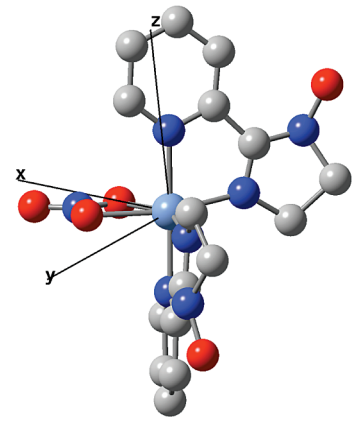

Figure 1. The $[Ni(HIM2-Py)_2NO_3]^+$] complex (**1**) and its proper magnetic axes. The magnetic *z*-axis has an angle of 12.7° with the normal of the plane formed by Ni and by the NO_3^- ligand.

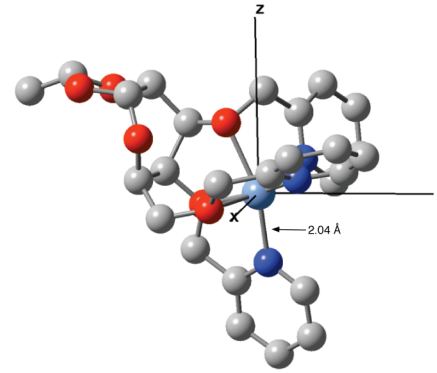

Figure 2. The $[Ni(glycoligand)]^{2+}$] complex (**2**) and its proper magnetic axes. The magnetic *z*-axis has an angle of 9.5° with the 2.04 Å Ni−N bond.

2. Methodological Study

2.1. Description of the Compounds and Computational Information. Three Ni(II) complexes and one Co(II) complex were studied. $[Ni(HIM2-Py)_2\ NO_3]^+$ (**1**, see Figure 1) and $[Ni(glycoligand)]^{2+}$ (**2**, see Figure 2) show a quasi-octahedral coordination of Ni(II), while [Ni(*i*Prtacn)Cl_2] (**3**, see Figure 3) has a pentacoordinated Ni(II) ion in an arrangement of the ligands that is intermediate between a trigonal bipyramid and a square pyramid. The geometries have been taken from crystallographic data and experimental information about the structure, high-field, high-frequency electron paramagnetic resonance (HF-HFEPR) and frequency domain magnetic resonance spectroscopy (FDMRS) data can be found in refs 46−48 for each compound, respectively. In order to reduce the computational cost for **1**, the CH_3 groups, which are geometrically distant from the metal ion, have been modeled

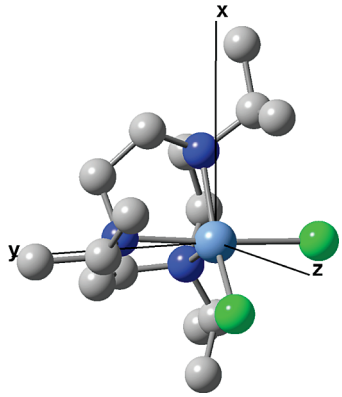

Figure 3. The [Ni(*i*Prtacn)Cl_2] complex (**3**) and its proper magnetic axes. The magnetic *z*-axis has an angle of 26.0° with the Cl−N−Cl plane.

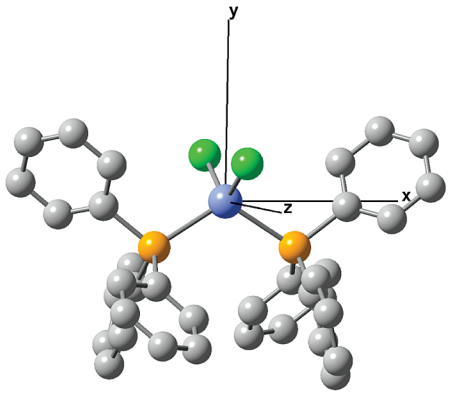

Figure 4. The [Co(PPh_3)$_2Cl_2$] (Ph = phenyl) complex (**4**) and its proper magnetic axes.

by H atoms. Owing to the local character of the ZFS property, this simplification should not affect the results. The local geometry of Co(II) in [Co(PPh_3)$_2Cl_2$][49,50] (**4**, see Figure 4), is a distorted tetrahedron.

The electronic structure of the complexes have been studied using the SO-RASSI method[51,52] implemented in MOLCAS 7. The scalar relativistic effects are included through the use of the Douglas−Kroll−Hess Hamiltonian,[53,54] and the SO effects are treated within the one-component formalism through the so-called spin-orbit state interaction (SO-SI) technique using the atomic mean-field approximation (AMFI). The method is a two-step procedure based on the idea that electron−correlation and SO effects are largely decoupled. The first step involves a complete active space self-consistent field (CASSCF) calculation to treat nondynamic correlations followed by the introduction of dynamic correlation effects through the evaluation of the single and double excitation contributions in a second-order perturbative manner (CASPT2). The second step calculates the SO interactions between the CASSCF states. The CASSCF diagonal elements of the so-obtained SO-SI matrix are substituted by the CASPT2 energies in order to take into account the main dynamic correlation effects.[55,56] In this method, the dipole-spin coupling is neglected. Contrarily to what was assumed for several decades, it has recently been shown that for Mn(III) complexes, the spin−spin part is not negligible for a quantitative description of the anisotropy.[22,10] In the considered Ni(II) and Co(II) complexes, the contribution of the SO interaction to the anisotropy is relatively important, and the number of unpaired electrons is small. Hence, the spin−spin part is expected to bring a minor contribution to the overall anisotropy.

Two different active spaces have been considered in the CASSCF calculations. The minimal active space has five TM-3d (TM = Ni,Co) orbitals and an extra set of five TM-d′ orbitals to accurately describe the radial electron correlation. This gives a CAS(8,10) and CAS(7,10) for the Ni- and Co-based compounds, respectively. The second, extended active space also includes some doubly occupied σ ligand−metal bonding orbitals. These orbitals essentially represent the nonbonding pairs of the atoms coordinated to the metal ion. Adding the orbitals with the strongest TM−ligand interaction leads to CAS(12,12) and CAS(13,13) for Ni- and Co-based compounds, respectively. Molecular orbitals have been optimized in an average way for all states belonging to a given spin multiplicity. The following all-electron ANO-RCC basis sets[57] are used: Ni and Co (6s 5p 4d 2f), Cl and P (5s 4p 1d), coordinated N (4s 3p 1d), other N (3s 2p 1d), O (4s 3p 1d), C (3s 2p), and H (2s).

The IP-EA shift has been set to zero for the nickel complexes since the states which are strongly coupled through the SO interaction are the lowest triplets, which have the same number of unpaired electrons, and to 0.25 for the cobalt one for which the excited doublets were suspected to play an important role. The minimal imaginary shift necessary in order to remove intruder states has been introduced in all cases (0.05 for **1** and **2**, 0.10 for **3,** and 0.20 au for **4**).

2.2. Dependence of the Zero-Field Splitting on the Computational Degrees of Freedom of the SO-RASSI Method. In addition to the usual computational degrees of freedom, such as the number of basis functions and the size of the active space, the outcomes of the SO-RASSI calculations also depend on the number of states included in the state interaction and the choice of the diagonal elements in the SO matrix: CASSCF or CASPT2 energies. To establish the precision of the SO-RASSI method, we explored these computational degrees of freedom in **1** and **4**. We concentrated on three aspects: (i) the number of excited states, which are included in the SO-SI space. Here a balance should be found between the computational cost of calculating many excited states and the influence of the matrix elements on the final result; (ii) The size of the active space, i.e. the effect of the inclusion of the ligand-to-metal charge transfer excitations in the CASSCF wave function affect the low-energy spectrum; and (iii) the comparison of the results using CASSCF or CASPT2 energies on the diagonal of the SO-SI matrix.

The dependence of the results to the number of states considered in the SO-SI calculations is studied for compounds **1** and **4**. The number of states has progressively been reduced starting from the complete TM-3d^n manifold to finally four states only. The selection of the states is based on an energy criterion, and states which are close in energy are removed from the SO-SI space simultaneously. In both cases, the smallest calculations (four states) couples the ground state with the first three excited states. These three states correspond to the three degenerate spatial components

Table 1. Energy Differences (in cm^{-1}) of the Spin−Orbit Splitted States Arising from the Fundamental Triplet State of **1** as Function of the Number of Spin−Orbit Coupled States[a]

		ΔE_1		ΔE_2	
number of states in SI	active space	CASSCF	CASPT2	CASSCF	CASPT2
10T, 14S	(8,10)	15.1	11.6	13.2	10.1
10T, 9S	(8,10)	17.1	14.2	14.5	11.7
7T, 2S	(8,10)	14.1	10.7	12.4	9.3
4T	(8,10)	14.8	13.0	13.0	11.3
4T	(12,12)	12.9	11.4	11.3	9.8
FDMRS[46]		10.3 ± 0.1		9.7 ± 0.1	

[a] $\Delta E_1 = E(|1,0\rangle) - E(|1,1\rangle - |1,-1\rangle)$ and $\Delta E_2 = E(|1,0\rangle) - E(|1,1\rangle + |1,-1\rangle)$. The number and spin multiplicity of the coupled states are indicated as *n*T(triplets) and *m*S(singlets).

Table 2. Energy Differences (in cm^{-1}) of the Spin−Orbit Splitted States Arising from the Fundamental Quartet State of **4** as Function of the Number of Spin−Orbit Coupled States[a]

		ΔE	
number of states in SI	active space	CASSCF	CASPT2
10Q, 40D	(7,10)	36.0	42.6
7Q	(7,10)	29.0	35.8
7Q	(13,13)	22.7	29.7
4Q	(7,10)	17.9	26.0
4Q	(13,13)	14.4	21.6
HF-HFEPR[49,50]		29.8	

[a] ΔE is the absolute value of $E(|3/2,\pm 3/2\rangle) - E(|3/2,\pm 1/2)$. The number and spin multiplicity of the coupled states are indicated as *n*Q (quartets) and *m*D (doublets).

of the first excited state in an ideal octahedral (Ni) or tetrahedral (Co) coordination. A further reduction of the SO-SI space is physically not grounded and has not been performed.

The d^8 configuration of the Ni(II) ion contains 25 spin free states, 10 triplets, and 15 singlets. Due to an intruder state problem, the CASPT2 energy of the highest singlet state could not be obtained with a high enough precision, hence 14 singlets have been considered in the SO calculation. Since this last singlet is very high in energy, its neglect is not expected to have any significant influence on the ZFS parameters. The Co(II)-d^7 configuration contains 10 quadruplets and 40 doublets. In this case, the energetic decomposition is not trivial since, except for the seven first quadruplet states which are well separated in energy from the others, all the other excited states are close in energy. We have, therefore, only compared the results obtained for the four and seven quadruplets and the complete collection of the 50 states of the configuration.

Table 1 compares the computed relative energies of the M_S components (or their combinations) of the ground state of **1** to the experimental ones for different SO-SI spaces. Table 2 lists the energy difference of the lowest two Kramers doublets for **4**. In all cases, the states are labelled using the main M_S components (or their combinations) appearing in the SO wave functions computed in the proper magnetic axes frame (the determination of this frame is discussed in Section 3). FDMRS transition energies are available for compound **1**, while the transition energy has been calculated from the ZFS parameters derived from the EPR data for **4**.

From the results reported in Tables 1 and 2, several conclusions can be inferred:

(i) In the Ni compounds, the lowest excited states of the same spin multiplicity as the ground state, i.e., the three lowest excited triplets, make the main contribution to ZFS. The analysis of the physical content of the wave functions of these SO excited states rationalizes their predominant role. They all result from a single electron replacement in the TM-3d orbitals with respect to the fundamental state. These excited states are, therefore, not only low in energy but also strongly coupled through SO coupling with the ground state. For the quasi-tetrahedrally coordinated Co complex, the SO-SI space cannot be restricted to the lowest four quartet states, which arise from the $^4A_2$ and $^4T_2$ states of the perfect tetrahedron. The three excited states arising from the $^4T_1$ state are so low in energy that they have a non-negligible interaction via the SO operator with the ground state, notwithstanding the marked contribution of the doubly excited configurations in the wave functions of these states.

(ii) At first sight, it may be surprising that the best agreement with experiment is obtained for the smaller SO-SI spaces (4T for **1** and 7Q for **4**), and that the inclusion of more states does not improve the result or even worsen it. However, the use of the state-average CASSCF orbitals to obtain the higher excited states affects the description of the lowest states. Indeed, in these averaged orbital sets, these states are less precisely described than in a set of orbitals optimized for the lowest states only. Hence, the precision that is gained by enlarging the SO-SI space is lost by the more approximate description of the lowest excited states. This is a limitation of the CASPT2/SO-SI methodology, enlarging the SI space does not guarantee a convergence of the results. Hence, we would recommend to optimize the orbitals in an average way for only those states that strongly interact through the SO coupling with the ground state.

(iii) Reasonable results can be obtained with a relatively small computational effort. Qualitative agreement with experiment is observed for the CASSCF wave functions and the energies calculated with the smaller active space, averaging for the lowest electronic states only. The incorporation of dynamic correlation effects (CASPT2) moderately modifies the obtained results. For a quantitative agreement with experiment, it is necessary to extend the active space to those ligand orbitals that have sizable tails on the metal center. This shows that the ligand-to-metal charge transfer (LMCT) configurations can play an important role in the magnetic anisotropy and should be variationally described. The active space should be chosen in such a way that it does not only include the radial electron correlation (smaller active space) but also the nondynamical correlation effects associated to the LMCT configurations.

3. Theory and Results

3.1. General Approach. The model spin Hamiltonian of a mononuclear anisotropic complex in the absence of a magnetic field is given by the following expression:

$$\hat{H}^{\mathrm{mod}} = \hat{S} \cdot \bar{\bar{D}} \cdot \hat{S} \quad (1)$$

where $\hat{S}$ is the spin operator, and $\bar{\bar{D}}$ is the second-order anisotropy tensor. For more than three unpaired electrons, even higher-order terms can be considered in the model Hamiltonian.[43] These higher-order terms will not be considered here since the complexes studied are limited to two or three unpaired electrons only. The projections of the lowest SO states onto the $|S,M_S\rangle$ states constitute the basis functions of the model space S_0 on which this model Hamiltonian is spanned. The SO coupling results in a mixing of the M_S components and, therefore, in a removal of their degeneracy. The procedure to extract the ZFS tensor, which is proposed here, uses the effective Hamiltonian theory.[58,59] This theory is based on the existence of a biunivocal relation between a model space S_0 and a target space S constituted of those eigenstates Ψ_i of the all-electron Hamiltonian that should be accurately reproduced by the model Hamiltonian. The effective Hamiltonian (which will be later compared to the model Hamiltonian) may be written as

$$\hat{H}^{\mathrm{eff}} = \sum_i |\tilde{\Psi}_i\rangle E_i \langle\tilde{\Psi}_i| \quad (2)$$

where $|\tilde{\Psi}_i\rangle$ are the orthogonalized projections of the $|\Psi_i\rangle$ states onto S_0, and E_i are their ab initio energies. The projections were orthogonalized by an $S^{-1/2}$ orthonormalization (where S is the overlap matrix) as proposed by des Cloizeaux.[59] This formalism guarantees that the eigenvalues of the model Hamiltonian are the eigenvalues of the all-electron Hamiltonian, and that its eigenfunctions are the orthogonalized projections $|\tilde{\Psi}_i\rangle$ of the eigenfunctions of the all-electron Hamiltonian onto the model space, such that:

$$\hat{H}^{\mathrm{eff}}|\tilde{\Psi}_i\rangle = E_i|\tilde{\Psi}_i\rangle \quad (3)$$

The norm of these projections provides a rational way to check the relevance of the model Hamiltonian to be extracted. If the norm of the projection is small, then important physics are missing in the model space, and one should reconsider the definition of the model Hamiltonian. Therefore, the method provides a rigorous and controlled way to extract the model Hamiltonian. Another advantage of the use of the effective Hamiltonian theory resides in the possibility to determine the principal axes of the ZFS tensor. Indeed, the expressions of both the eigenfunctions of the all-electron Hamiltonian and the matrix elements of the effective Hamiltonian defined in eq 2 depend on the axes frame. An identification of these terms with those of the analytical matrix of the model Hamiltonian expressed in the general case of a nondiagonal tensor leads to a complete determination of the $\bar{\bar{D}}$ components in an arbitrary frame. The proper magnetic axes are then determined from the diagonalization of the ZFS tensor. In comparison to the perturbative approach of calculating the ZFS tensor components, the effective Hamiltonian theory enables one to identify as high-order terms as required, since the interactions of the model Hamiltonian (and therefore its operators) are not guessed a priori. To recover the results of the effective Hamiltonian theory, one should expand the perturbation until an infinite order.

3.2. Extraction of the ZFS Parameters from the Effective Hamiltonian Theory. The ZFS tensor is only diagonal in the magnetic anisotropy axes frame. In the following development, its matrix representation in an arbitrary frame will be denoted as

$$\mathbf{D} = \begin{pmatrix} D_{11} & D_{12} & D_{13} \\ D_{12} & D_{22} & D_{23} \\ D_{13} & D_{23} & D_{33} \end{pmatrix} \quad (4)$$

The elements of the analytical matrix of $\hat{H}^{\mathrm{mod}}$ (eq 1) are functions of the different components D_{ij}, including the extradiagonal elements of the ZFS tensor. Using $|1,-1\rangle$, $|1,0\rangle$, and $|1,1\rangle$ as basis functions, the matrix elements $\langle S,M_S|\hat{H}^{\mathrm{mod}}|S,M'_S\rangle$ for the high spin d^8 configuration are

$\hat{H}_{\mathrm{mod}}$	$\lvert 1,-1\rangle$	$\lvert 1,0\rangle$	$\lvert 1,1\rangle$
$\langle 1,-1\rvert$	$\frac{1}{2}(D_{11}+D_{22})+D_{33}$	$-\frac{\sqrt{2}}{2}(D_{13}+iD_{23})$	$\frac{1}{2}(D_{11}-D_{22}+2iD_{12})$
$\langle 1,0\rvert$	$-\frac{\sqrt{2}}{2}(D_{13}-iD_{23})$	$D_{11}+D_{22}$	$\frac{\sqrt{2}}{2}(D_{13}+iD_{23})$
$\langle 1,1\rvert$	$\frac{1}{2}(D_{11}-D_{22}-2iD_{12})$	$\frac{\sqrt{2}}{2}(D_{13}-iD_{23})$	$\frac{1}{2}(D_{11}+D_{22})+D_{33}$

(5)

The next step is the construction of the effective Hamiltonian based on the ab initio calculations. We take here, as an example, the CAS(12,12)PT2 results of **1** with the 4T SO-SI space (one but last row in Table 1). The projections of the eigenfunctions all electron Hamiltonian on the model space at this level of calculation are

$$|\tilde{\Psi}_1\rangle = (0.045 + 0.092i)|1,-1\rangle + (-0.668 + 0.724i)|1,0\rangle + (0.096 + 0.037i)|1,1\rangle$$
$$|\tilde{\Psi}_2\rangle = (-0.395 + 0.578i)|1,-1\rangle + (0.062 + 0.088i)|1,0\rangle + (-0.678 + 0.173i)|1,1\rangle$$
$$|\tilde{\Psi}_3\rangle = (0.701 + 0.026i)|1,-1\rangle + (-0.090 - 0.037i)|1,0\rangle + (-0.519 - 0.472i)|1,1\rangle$$

Using these projections and the corresponding energy eigenvalues ($E_1 = 0.000$, $E_2 = 1.529$, $E_3 = 11.369$ cm^{-1}), the application of eq 2 leads to the following numerical effective Hamiltonian:

	$\lvert 1,-1\rangle$	$\lvert 1,0\rangle$	$\lvert 1,1\rangle$
$\langle 1,-1\rvert$	6.386	$-0.690 + 0.376i$	$-3.734 + 3.134i$
$\langle 1,0\rvert$	$-0.690 - 0.376i$	0.125	$0.690 - 0.376i$
$\langle 1,1\rvert$	$-3.734 - 3.134i$	$0.690 + 0.376i$	6.386

(6)

Before calculating the ZFS tensor **D**, we observe that there is a perfect one-to-one correspondence of the matrix elements of the effective Hamiltonian derived from the ab initio calculations and those of the model Hamiltonian of eq 5. The effective Hamiltonian does not present extra interaction to those expected from the model Hamiltonian. Combined with the large norm of the projections, we conclude that the model Hamiltonian (eq 1) perfectly describes the ZFS in this case. The same behavior is found for the other Ni(II) compounds. The comparison of eqs 5 and 6 leads to six linear independent equations in terms of the D_{ij}, which determine uniquely the ZFS tensor. The full expression of the numerical effective Hamiltonians for **2** and **3** can be found in the

Supporting Information. From eqs 5 and 6 we derive the values of the **D** tensor of **1** in the original coordinates frame.

$$\mathbf{D} = \begin{pmatrix} -3.671 & 3.134 & 0.976 \\ 3.134 & 3.797 & -0.532 \\ 0.976 & -0.532 & 6.323 \end{pmatrix} \tag{7}$$

The **D** tensors for **2** and **3** are given in the Supporting Information. The diagonalization of **D** gives us the transformation matrix to rotate the coordinates frame such that the axes coincide with the magnetic one. These axes are indicated in the Figures 1−3 for the complexes studied here. Note that the orientation of the magnetic axes is almost independent of the computational degrees of freedom, unlike the energy differences between the lowest spin−orbit states, as shown in the previous section. Furthermore, it allows us to determine the commonly used ZFS parameters for the axial ($D = (3/2)D_{zz}$) and the rhombic ($E = (1/2)(D_{xx} - D_{yy}) > 0$) anisotropy. In the general case presented here, (Tr $\mathbf{D} \neq 0$), D and E can be derived from

$$\begin{aligned} D &= D_{33} - \frac{1}{2}(D_{11} + D_{22}) \\ E &= \frac{1}{2}(D_{11} - D_{22}) > 0 \end{aligned} \tag{8}$$

In practice, D_{33} is chosen as the diagonal element that maximizes the spacing with respect to the other two diagonal elements. D_{11} and D_{22} are identified by the convention that E is always positive. The resulting anisotropy parameters for **1**−**3** are listed in Table 3 and will be discussed in the next section.

For the Ni(II) complexes, the ZFS parameters can, of course, also be extracted from the spectrum only without going through the construction of the effective Hamiltonian. One should notice, however, that the magnetic anisotropy axes could not be determined, and that no information about the character of the wave functions can be used.

3.3. Extraction of ZFS Parameters for the d^7 Configuration. Spin−orbit interaction splits the quartet ground state of the high spin d^7 configuration into two Kramers doublets. Hence, the information from the spectrum is obviously not enough to determine the ZFS parameters D and E. It is not even possible to determine the sign of the axial anisotropy, except for the case when the magnetic axes are known and the wave function is available. This is, however, generally not the case, and the construction of an effective Hamiltonian is the preferred route toward a full description of the ZFS. Following the previously outlined procedure, we first calculate the matrix elements of the model Hamiltonian in the $|S,M_S\rangle$ basis for the d^7 configuration:

$$\begin{array}{c|cccc} \hat{H}_{\mathrm{mod}} & \left|\frac{3}{2},-\frac{3}{2}\right\rangle & \left|\frac{3}{2}-\frac{1}{2}\right\rangle & \left|\frac{3}{2},\frac{1}{2}\right\rangle & \left|\frac{3}{2},\frac{3}{2}\right\rangle \\ \left\langle\frac{3}{2},-\frac{3}{2}\right| & \frac{3}{4}(D_{11}+D_{22})+\frac{9}{4}D_{33} & -\sqrt{3}(D_{13}+iD_{23}) & \frac{\sqrt{3}}{2}(D_{11}-D_{22}+2iD_{12}) & 0 \\ \left\langle\frac{3}{2},-\frac{1}{2}\right| & -\sqrt{3}(D_{13}-iD_{23}) & \frac{7}{4}(D_{11}+D_{22})+\frac{1}{4}D_{33} & 0 & \frac{\sqrt{3}}{2}(D_{11}-D_{22}+2iD_{12}) \\ \left\langle\frac{3}{2},\frac{1}{2}\right| & \frac{\sqrt{3}}{2}(D_{11}-D_{22}-2iD_{12}) & 0 & \frac{7}{4}(D_{11}+D_{22})+\frac{1}{4}D_{33} & \sqrt{3}(D_{13}+iD_{23}) \\ \left\langle\frac{3}{2},\frac{3}{2}\right| & 0 & \frac{\sqrt{3}}{2}(D_{11}-D_{22}-2iD_{12}) & \sqrt{3}(D_{13}-iD_{23}) & \frac{3}{4}(D_{11}+D_{22})+\frac{9}{4}D_{33} \end{array} \tag{9}$$

Subsequently, the effective Hamiltonian is constructed from the ab initio energies and wave functions. The numerical expression of this Hamiltonian can be found in the Supporting Information. We note again that the model Hamiltonian perfectly fits the effective Hamiltonian, and hence, the full **D** tensor can be extracted. The magnetic axes are shown in Figure 4, and the ZFS parameters are listed in Table 3. The appearance of off-diagonal terms in the effective Hamiltonian suggests that the eigenfunctions can have contributions from determinants with different M_S values. This implies that M_S is not a good quantum number anymore. Nevertheless, the off-diagonal terms that cause the interaction between the determinants with different M_S values are strictly zero in the proper magnetic frame under the condition of no rhombic distortion. In the case of **4**, the rhombic distortions are small ($E/|D| = 0.08$), and the wave functions that describe the four lowest states have almost pure $M_S = \pm 1/2$ or $M_S = \pm 3/2$ character.

3.4. Magneto-Structural Relations for *D* and *E*. Table 3 compares the calculated anisotropy parameters with the experimental values of these parameters extracted from HF-HFEPR data.[46−49] While the agreement with experiment is excellent for **1**, **3**, and **4**, the calculated D-value for **2** deviates by approximately 4 cm^{-1}. The smallness of the anisotropy of this complex may be the origin of the difference between theory and experiment. The SO-SI methodology may have reached its numerical precision for this complex. This is subject to further study on other complexes with small anisotropy.

A less equally important question is whether it can be established why **1** has a large negative D, **2** a very small D, and **3** a large positive D. For this purpose, we study the effect of different distortions on the anisotropy in the three Ni(II) complexes using CASSCF energies and the 4T SO-SI space. The starting point for the decomposition is the isotropic, perfect octahedron of the model compound $[Ni(NCH)_6]^{2+}$. The first coordination sphere of complex **1** shows two major distortions in the xy-plane. The first distortion is a cis elongation, and the second is an angular distortion in which one N−Ni−N angle increases to

Table 3. SO-SI Axial and Rhombic Anisotropy Parameters D and E (in cm^{-1}) for Three Ni(II) Complexes (**1**−**3**) and One Co(II) Complex (**4**)[a]

	SO-SI		exptl	
complex	D	E	D	E
1	−10.60	0.76	−10.15	0.10
2	8.10	0.58	4.40	0.75
3	16.45	3.82	15.70	3.40
4	−14.86	0.54	−14.76	1.14

[a] Calculations were performed with the extended CAS and the 4T or 7Q SO-SI space for **1**−**3** and **4**, respectively. The energies of the spin-free states are calculated with CASPT2.

100° and the opposite angle reduces to 60°. Other smaller distortions complete the route from perfect octahedron to real geometry. The subsequent application of these three distortions gives $D = +0.2$ cm^{-1} (*xy*-plane elongation), $D = -4.9$ cm^{-1} (after adding the angular distortion), and $D = -9.6$ cm^{-1} for the complete distortion. Hence, the largest effect on the anisotropy is found to be the *xy*-plane angular distortion, while the combination of the smaller angular distortions significantly enhances the D parameter.

The geometry of **2** is close to octahedral, showing an elongation along the positive *z*-axis and an angular distortion of both axial ligands in cis mode. Applying these distortions on the model complex gives $D = +3.0$ cm^{-1} for the elongation and $D = -4.5$ cm^{-1} for the axial distortion. The application of both distortions simultaneously gives $D = +6.1$ cm^{-1}, close to the value calculated for the real complex.

Complex **3** is pentacoordinated. Hence, the first obvious distortion is the removal of one of the ligands from the model complex. The resulting square pyramid leads to a large positive D of $+16.3$ cm^{-1}, while the trigonal bypiramid leads to a first-order angular momentum in the ground state, and the model Hamiltonian, which only contains spin operators, no longer applies. On the way to the real geometry, we apply an elongation of two equatorial cis ligands on the square pyramid, reducing the D-value to $+11.2$ cm^{-1}. The next distortion that should be applied is an angular out-of-plane distortion of 60° from one the equatorial ligands. This causes, again, a near degeneracy and an appearance of a first-order angular momentum. Alternatively, we constructed a $[Ni(NCH)_5]^{2+}$ model with the same geometry as the first coordination sphere as the real complex **3**. This resulted in a D-value of $+24.4$ cm^{-1}. After replacing two NCH groups by Cl ligands, as in the real complex, D further increases to $+27.7$ cm^{-1}. The only remaining difference with the real complex is the replacement of the three NCH ligands with *i*Prtacn, which reduces the anisotropy to $D = +20$ cm^{-1}. This demonstrates the important interplay between the geometry and the σ-donating character of the ligands in the anisotropy of the complex, whose character is mainly determined by its resemblance to the square pyramid.

4. Conclusions

From the wave functions and the energies of the all-electron Hamiltonian, effective Hamiltonian theory rigorously determines the anisotropic spin Hamiltonian of anisotropic monometallic compounds. The method gives access to all the components of the ZFS tensor and, therefore, leads to the extraction of both the axial D and the rhombic E anisotropy parameters and to the proper magnetic axes frame.

The advantages of the proposed method of extraction are most obvious for the high spin Co(II) compound for which the anisotropy parameters cannot be extracted from the relative energies of the lowest spin−orbit states.

The extracted D and E parameters are in good agreement with the HF-HFEPR data for large magnetic parameters, establishing the precision of the SO-SI method to describe single-ion anisotropy. The main conclusions of the methodological study are that the best results are obtained with wave functions and energies obtained from an enlarged active space that includes ligand orbitals.

Finally, the effective Hamiltonian theory permits the accuracy of the model Hamiltonian to reproduce the physics of the studied systems to be checked. In the present case, the validity of the usual Hamiltonian is confirmed for the d^7 and the d^8 configurations of monometallic complexes. The procedure is now being applied to other d^n configurations and to polymetallic systems in order to extract the interactions of both multispin and giant spin Hamiltonians.

Acknowledgment. We thank Carmen J. Calzado for providing us the basis for the effective Hamiltonian program. Financial support has been provided by the Spanish Ministry of Science and Innovation (Project CTQ2008-06644-C02-01) and the Generalitat de Catalunya (Project 2009SGR462 and Xarxa d'R+D+I en Química Teorica i Computacional, XRQTC). This work was supported by the French Centre National de la Recherche Scientifique (CNRS), Université de Toulouse.

Supporting Information Available: Numerical expression of the effective Hamiltonians for **1**, **2**, and **4**, **D**-tensors for **2**, **3**, and **4**, and orthogonalized projections of the ab initio wave function of **1** on the model space. This material is available free of charge via the Internet at http://pubs.acs.org.

References

(1) Caneschi, A.; Gatteschi, D.; Sessoli, R.; Barra, A. L.; Brunel, L. C.; Guillot, M. *J. Am. Chem. Soc.* **1991**, *113*, 5873.

(2) Friedman, J. R.; Sarachik, M. P.; Tejada, J.; Ziolo, R. *Phys. Rev. Lett.* **1996**, *76*, 3830.

(3) Thomas, C.; Lionti, F.; Ballou, R.; Gatteschi, D.; Sessoli, R.; Barbara, B. *Nature* **1996**, *383*, 145.

(4) Gatteschi, D.; Sessoli, R. *Angew. Chem., Int. Ed.* **2003**, *42*, 246.

(5) Gatteschi, D.; Sessoli R.; Villain J. *Molecular Nanomagnets*; Oxford University Press: Oxford, U.K., 2006.

(6) Neese, F. *ORCA*, Version 2.6; an ab initio, density functional and semiempirical program package; University of Bonn: Bonn, Germany, 2008.

(7) Sinnecker, S.; Neese, F.; Noodleman, L.; Lubitz, W. *J. Am. Chem. Soc.* **2004**, *126*, 2613.

(8) Neese, F.; Solomon, E. I. *Inorg. Chem.* **1998**, *37*, 6568.

(9) Ganyushin, D.; Neese, F. *J. Chem. Phys.* **2006**, *125*, 024103.

(10) Neese, F. *J. Am. Chem. Soc.* **2006**, *128*, 10213.

(11) Neese, F. *J. Chem. Phys.* **2007**, *127*, 164112.

(12) Pederson, M. R.; Khanna, S. N. *Phys. Rev. B: Condens. Matter* **1999**, *60*, 9566.

(13) Kortus, J.; Pederson, M. R.; Baruah, T.; Bernstein, N.; Hellberg, C. S. *Polyhedron* **2003**, *22*, 1871.

(14) Postnikov, A. V.; Kortus, J.; Pederson, M. R. *Phys. Status Solidi B* **2006**, *128*, 9497.

(15) Jackson, K. A.; Pederson, M. R. *Phys. Rev. B: Condens. Matter* **1990**, *42*, 3276.

(16) Pederson, M. R.; Jackson, K. A. *Phys. Rev. B: Condens. Matter* **1990**, *41*, 7453 (see also: http://cst-www.nrl.navy.mil/users/nrlmol).

(17) Reviakine, R.; Arbuznikov, A.; Tremblay, J. C.; Remenyi, C.; Malkina, O.; Malkin, V. G.; Kaupp, M. *J. Phys. Chem.* **2006**, *125*, 054110.

(18) Malkin, V. G.; Malkina, O. L.; Reviakine, R. *RESPECT Program*, Version 2.1, 2005. The property part of the code (MAG-ReSpect) is freely available as binary for LINUX PCs from the authors (vladimir.malkin@savba.sk).

(19) Ruiz, E.; Cirera, J.; Cano, J.; Alvarez, S.; Loose, C.; Kortus, J. *Chem. Commun.* **2008**, *1*, 52.

(20) Loose, C.; Ruiz, E.; Kersting, B.; Kortus, J. *Chem. Phys. Lett.* **2008**, *452*, 38.

(21) Havlas, Z.; Downing, J. W.; Michl, J. *J. Phys. Chem. A* **1998**, *102*, 5681.

(22) Engström, M.; Vahtras, O.; Ågren, H. *Chem. Phys. Lett.* **2000**, *328*, 483.

(23) Karlström, G.; Lindh, R.; Malmqvist, P.-Å.; Roos, B. O.; Ryde, U.; Veryazov, V.; Widmark, P.-O.; Cossi, M.; Schimmelpfennig, B.; Neogrady, P.; Seijo, L. *Comput. Mater. Sci.* **2003**, *28*, 222.

(24) Chibotaru, L.; Ungur, L.; Soncini, A. *Angew. Chem., Int. Ed.* **2008**, *120*, 4194.

(25) Petit, S.; Pilet, G.; Luneau, D.; Chibotaru, L. F.; Ungur, L. *Dalton Trans.* **2007**, 4582.

(26) Soncini, A.; Chibotaru, L. F. *Phys. Rev. B: Condens. Matter* **2008**, *77*, 220406.

(27) Chibotaru, L. F.; Ungur, L.; Aronica, C.; Elmoll, H.; Pilet, G.; Luneau, D. *J. Am. Chem. Soc.* **2008**, *130*, 12445.

(28) Sousa, C.; de Graaf, C. *Int. J. Quantum Chem.* **2006**, *106*, 2470.

(29) Calzado, C. J.; Cabrero, J.; Malrieu, J. P.; Caballol, R. *J. Chem. Phys.* **2002**, *116*, 2728.

(30) Calzado, C. J.; Cabrero, J.; Malrieu, J. P.; Caballol, R. *J. Chem. Phys.* **2002**, *116*, 3985.

(31) Calzado, C. J.; Malrieu, J. P. *Phys. Rev. B: Condens. Matter* **2001**, *63*, 214520.

(32) Bordas, E.; de Graaf, C.; Caballol, R.; Calzado, C. J. *Phys. Rev. B: Condens. Matter* **2005**, *71*, 045108.

(33) Guihéry, N.; Malrieu, J. P. *J. Chem. Phys.* **2003**, *119*, 8956.

(34) Taratiel, D.; Guihéry, N. *J. Chem. Phys.* **2004**, *121*, 7127.

(35) Bastardis, R.; Guihéry, N.; de Graaf, C. *Phys. Rev. B: Condens. Matter* **2006**, *74*, 014432.

(36) Guihéry, N. *Theor. Chem. Acc.* **2006**, *116*, 576.

(37) Bastardis, R.; Guihéry, N.; Suaud, N.; de Graaf, C. *J. Chem. Phys.* **2006**, *125*, 194708.

(38) Bastardis, R.; Guihéry, N.; Suaud, N. *Phys. Rev. B: Condens. Matter* **2007**, *75*, 132403.

(39) Bastardis, R.; Guihéry, N.; de Graaf, C. *Phys. Rev. B: Condens. Matter* **2008**, *77*, 054426.

(40) de P. R. Moreira, I.; Suaud, N.; Guihéry, N.; Malrieu, J. P.; Caballol, R.; Bofill, J. M.; Illas, F. *Phys. Rev. B: Condens. Matter* **2002**, *66*, 134430.

(41) Bastardis, R.; Guihéry, N.; de Graaf, C. *Phys. Rev. B: Condens. Matter* **2007**, *76*, 132412.

(42) Calzado, C. J.; de Graaf, C.; Bordas, E.; Caballol, R.; Malrieu, J. P. *Phys. Rev. B: Condens. Matter* **2003**, *67*, 132409.

(43) Boča, R. *Theoretical Foundations of Molecular Magnetism*; Elsevier: Amsterdam, The Netherlands, 1999, 642−680.

(44) Boča, R. *Coord. Chem. Rev.* **2004**, *248*, 757.

(45) Park, K. N.; Pederson, M. R.; Richardson, S. L.; Aliaga-Alcalde, N.; Christou, G. *Phys. Rev. B: Condens. Matter* **2003**, *68*, 020405.

(46) Rogez, G.; Rebilly, J. N.; Barra, A. L.; Sorace, L.; Blondin, G.; Kirchner, N.; Duran, M.; Van Slageren, J.; Parsons, S.; Ricard, L.; Marvilliers, A.; Mallah, T. *Angew. Chem., Int. Ed.* **2005**, *44*, 1876.

(47) Charron, G.; Bellot, F.; Cisnetti, F.; Pelosi, G.; Rebilly, J. N.; Riviere, E.; Barra, A. L.; Mallah, T.; Policar, C. *Chem. Eur. J.* **2007**, *13*, 2774.

(48) Rebilly, J. N.; Charron, G.; Riviere, E.; Guillot, R.; Barra, A. L.; Serrano, M. D.; Van Slageren, J.; Mallah, T. *Chem. Eur. J.* **2008**, *14*, 1169.

(49) Krzystek, J.; Zvyagin, S. A.; Ozarowski, A.; Fiedler, A. T.; Brunold, T. C.; Tesler, J. *J. Am. Chem. Soc.* **2004**, *126*, 2148.

(50) Carlin, R. L.; Chirico, R. D.; Sinn, E.; Mennenga, G.; de Jongh, L. J. *Inorg. Chem.* **1982**, *21*, 2218.

(51) Malmqvist, P.-Å.; Roos, B. O. *Chem. Phys. Lett.* **1989**, *155*, 189.

(52) Malmqvist, P.-Å.; Roos, B. O.; Schimmelpfennig, B. *Chem. Phys. Lett.* **2002**, *357*, 230.

(53) Douglas, N.; Kroll, N. M. *Ann. Phys.* **1974**, *82*, 89.

(54) Hess, B. *Phys. Rev. A: At., Mol., Opt. Phys.* **1986**, *33*, 3742.

(55) Llusar, R.; Casarrubios, M.; Barandiarán, Z.; Seijo, L. *J. Chem. Phys.* **1996**, *105*, 5321.

(56) Baradiarán, Z.; Seijo, L. *J. Chem. Phys.* **2003**, *118*, 7439.

(57) Roos, B. O.; Lindh, R.; -Å.; Malmqvist, P.; Veryazov, V.; Widmark, P. O. *J. Phys. Chem. A* **2005**, *109*, 6575.

(58) Bloch, C. *Nucl. Phys.* **1958**, *6*, 329.

(59) des Cloizeaux, J. *Nucl. Phys.* **1960**, *20*, 321.

CT900326E